

DCDT2980S, an Anti-CD22-Monomethyl Auristatin E Antibody–Drug Conjugate, Is a Potential Treatment for Non-Hodgkin Lymphoma

Dongwei Li¹, Kirsten Achilles Poon¹, Shang-Fan Yu¹, Randall Dere¹, MaryAnn Go¹, Jeffrey Lau¹, Bing Zheng¹, Kristi Elkins¹, Dimitry Danilenko¹, Katherine R. Kozak¹, Pamela Chan¹, Josefa Chuh¹, Xiaoyan Shi¹, Denise Nazzari¹, Franklin Fuh¹, Jacqueline McBride¹, Vanitha Ramakrishnan¹, Ruth de Tute^{2,3}, Andy Rawstron^{2,3}, Andrew S. Jack³, Rong Deng¹, Yu-Waye Chu¹, David Dornan¹, Marna Williams¹, William Ho¹, Allen Ebens¹, Saileta Prabhu¹, and Andrew G. Polson¹

Abstract

Antibody–drug conjugates (ADC), potent cytotoxic drugs linked to antibodies via chemical linkers, allow specific targeting of drugs to neoplastic cells. We have used this technology to develop the ADC DCDT2980S that targets CD22, an antigen with expression limited to B cells and the vast majority of non-Hodgkin lymphomas (NHL). DCDT2980S consists of a humanized anti-CD22 monoclonal IgG1 antibody with a potent microtubule-disrupting agent, monomethyl auristatin E (MMAE), linked to the reduced cysteines of the antibody via a protease cleavable linker, maleimidocaproyl-valine-citrulline-p-aminobenzoyloxycarbonyl (MC-vc-PAB). We describe the efficacy, safety, and pharmacokinetics of DCDT2980S in animal models to assess its potential as a therapeutic for the treatment of B-cell malignancies. We did not find a strong correlation between *in vitro* or *in vivo* efficacy and CD22 surface expression, nor a correlation of sensitivity to free drug and *in vitro* potency. We show that DCDT2980S was capable of inducing complete tumor regression in xenograft mouse models of NHL and can be more effective than rituximab plus combination chemotherapy at drug exposures that were well tolerated in cynomolgus monkeys. These results suggest that DCDT2980S has an efficacy, safety, and pharmacokinetics profile that support potential treatment of NHL. *Mol Cancer Ther*; 12(7): 1255–65. ©2013 AACR.

Introduction

Malignancies of B-cell origin are a heterogeneous group of neoplasms, which vary in genetic drivers of transformation, B-cell subtype of origin, and clinical outcome (1). Major unmet medical needs for B-cell malignancies include non-Hodgkin lymphoma (NHL) and chronic lymphocytic leukemia (CLL). The subclasses of NHL range in clinical outcome from slow-growing indolent and incurable diseases with a median survival of 8 to 10 years, such as follicular non-Hodgkin lymphoma (2), to more aggressive intermediate- to high-grade lymphomas (such as diffuse large-cell lymphoma), which can have a median

survival of 6 months if left untreated or long-term remission in more than 50% of patients with appropriate treatment (3). Mantle cell lymphoma (MCL) shares characteristics of both types, being incurable with a short remission following treatment. Diffuse large B-cell lymphoma (DLBCL) is the most common type of NHL, accounting for approximately 30% to 40% of all new patients, whereas follicular lymphoma (FL) and MCL account for approximately 20 to 25% and 6 to 10% of new lymphomas, respectively. CLL is the most common chronic leukemia in adults with approximately 15,000 new cases per year in the United States (4) and like follicular lymphoma is indolent but incurable. Despite advances in the clinical outcomes of patients with NHL and CLL using treatments such as the CD20-specific monoclonal antibody rituximab (Rituxan, MabThera), indolent B-cell malignancies remain incurable as are approximately half of patients with aggressive NHL. Thus, there is an unmet medical need for new therapies that are preferably better tolerated than the current standards of care.

Previously we identified CD22 and CD79 as superior targets for antibody–drug conjugate (ADC), potent cytotoxic drugs linked to antibodies via chemical linkers, therapy for the treatment of NHL (5–7). CD22 is a 130 kDa type I transmembrane glycoprotein, normally expressed on B-lineage cells from the pre-B-cell stage,

Authors' Affiliations: ¹Research and Early Development, Genentech Inc., South San Francisco, California; ²Haematological Malignancy Diagnostic Service, Leeds Teaching Hospitals, Leeds; ³Hull York Medical School (HYMS), University of York, Heslington, York, United Kingdom

Note: Supplementary data for this article are available at Molecular Cancer Therapeutics Online (<http://mct.aacrjournals.org>).

D. Li, K.A. Poon, and S.-F. Yu contributed equally to this work.

Corresponding Author: Andrew G. Polson, Genentech Research and Early Development, 1 DNA Way, South San Francisco, CA 94080. Phone: 650-225-5134; Fax: 650-225-6240; E-mail: polson@gene.com

doi: 10.1158/1535-7163.MCT-12-1173

©2013 American Association for Cancer Research.

and to being fully expressed on all subtypes of mature B-cell and downregulated from the surface of plasma cell. CD22 is also expressed on most malignant mature B cells, including follicular NHL, marginal zone lymphoma (MZL), MCL, DLBCL, small lymphocytic lymphoma (SLL), and CLL (refs. 6, 8 and this article). CD22 is not expressed on non-B lymphoid cells including, myeloid cells, hematopoietic stem cells, or any other nonhematopoietic lineage thus making it an excellent target for antibody and ADC therapy for a wide range of B-cell malignancies (9). Antibodies and ADCs targeted to CD22 are being tested in clinical trials for efficacy in NHL. An unconjugated humanized anti-CD22 antibody, epratuzumab, is currently in clinical trials for the treatment of B-cell malignancies (10) and lupus (11). The ADC inotuzumab ozogamicin (IO, CMC-544) a human IgG4 monoclonal antibody to CD22 conjugated via an acid-labile hydrazone linker to a cytotoxic DNA-damaging agent calicheamicin (12, 13) is being tested in clinical trials for treatment of NHL. Both of these anti-CD22 therapeutics have shown efficacy and have not displayed major toxicities relating to the targeting of CD22.

In this article, we describe the efficacy, safety, and pharmacokinetics of the anti-CD22 ADC DCDT2980S in animal models. DCDT2980S consists of a humanized anti-CD22 monoclonal IgG1 antibody, MCDT2219A, with a potent antimetabolic chemotherapeutic agent, monomethyl auristatin E (MMAE) chemically linked to the reduced cysteines of the antibody via a protease labile linker, maleimidocaproyl-valine-citrulline-p-aminobenzoyloxy-carbonyl (MC-vc-PAB). We have investigated the efficacy and safety of DCDT2980S in animal models to assess its potential as a therapeutic for the treatment of B-cell malignancies.

Materials and Methods

Antibodies and ADCs

The antibody for DCDT2980S (MCDT2219A, Hu10F4) was generated and humanized as previously described (6). The antibody was conjugated as previously described (14). Briefly, ADCs were prepared by incubating the maleimido drug derivative with the partially reduced antibodies for 1 hour at 4°C. After quenching the reaction with excess *N*-acetyl-cysteine, to react with any free linker-drug, the conjugated antibody was purified. Conjugation conditions were chosen to achieve an average drug-to-antibody ratio (DAR) of approximately 3.5. ADC protein concentrations were calculated using absorbance at 280 nm (320 nm reference) and the molar extinction coefficient of the antibody. The average DARs were calculated from the integrated areas of the DAR species resolved by hydrophobic interaction chromatography (HIC) on an analytical column (TSK butyl-NPR 4.6 mm × 10 cm 2.5 mm, Tosoh Bioscience).

Cell lines

The NHL cell lines DOHH2, Granta-519, Karpas-1106P, MHH-PREB-1, NU-DUL-1, NU-DHL-1, Ramos,

RC-K8, REC-1, SC-1, SU-DHL-1, SU-DHL-4, SU-DHL-5, SU-DHL-6, SU-DHL-8, SU-DHL-10, SU-DHL-16, U-698-M, WSU-DLCL2, and WSU-NHL were obtained from DSMZ. The DB, Farage, HT, MC116, Pfeiffer, and Toledo cell lines were obtained from the American Type Culture Collection. The A4/Fukada, SCC-3, TK were obtained from JHSF. All cell lines were maintained in RPMI-1640 supplemented with 10% FBS (Sigma) and 2 mmol/L L-glutamine. Each cell line authenticated by short tandem repeat (STR) profiling using the Promega PowerPlex 16 System and compared with external STR profiles of cell lines to determine cell line ancestry. In addition, a single-nucleotide polymorphism (SNP) fingerprint is generated from the original thaw to serve as our internal master fingerprint. The SNP fingerprinting is conducted each time a new batch is frozen down. Cell lines were typically used for several months before thawing a new passage.

CD22 expression levels in xenograft tumors

To measure the CD22 expression on xenograft tumors, recovered tumors were minced and put through a 30 μm cell strainer (BD Biosciences) to achieve a single-cell suspension. The tumor cells were subsequently prepared by the standard density centrifugation over lymphocyte separation medium (MP Biomedical). The resulting single-cell suspension was stained with anti-human CD22-APC antibody (BD Biosciences, clone S-HCL-1), anti-human CD20- Pacific Blue (Beckman Coulter), and 7-amino-actinomycin D (BD Biosciences). Data were analyzed using FlowJo (Tree Star), and the mean fluorescent intensity (MFI) was calculated from the CD20⁺ and 7-amino-actinomycin D⁻ population. CD22 expression on cell lines was measured with the same CD22-APC antibody.

CD22 expression levels in patient tumors

Tissue biopsies were dissociated using a needle and syringe. FACSFlow (10 mL; BD Biosciences, cat. no. 342003) was injected into the biopsy to flush leucocytes from the mass. Leucocytes from tissue, bone marrow aspirates, and peripheral blood were all then prepared using ammonium chloride lysis to remove red cells. A volume of sample was incubated with a 10-fold excess of ammonium chloride (8.6 g/L in distilled H₂O, Vickers Laboratories, Pudsey, United Kingdom; cat. no. 0055-CO) for 5 minutes at 37°C. Cells were then washed twice in buffer [FACSFlow containing 0.3% bovine serum albumin (Sigma; cat. no. A3059)]. Leucocytes (1 × 10⁶) were stained with 30 μL of a pre-prepared cocktail of antibodies. Samples were assayed using the panel of antibodies described. Following incubation in the dark at 4°C for 20 minutes, cells were washed twice in buffer and resuspended in FACSFlow. Samples were acquired on a FACS Canto II analyser using FACSDiva software (BD Biosciences). A minimum of 50,000 events were acquired for each tube of the panel.

Data analysis was carried out using FacsDiva software (Biosciences, Oxford). B cells were gated using CD19

PE-Cy5.5 (SJ25-C1), forward-scatter, and side-scatter parameters. Appropriate non-B-cell pan markers served as isotype controls for gating of positive and negative quadrants. CD8 APC (SK1) was used as an isotype control for CD22 APC (S-HCL-1). MFIs presented as normalized values (MFI CD22-MFI CD8).

Cell viability assay

Cells were plated in quadruplicate at 1 to 5×10^3 per well in 384-well plates in RPMI containing 10% FBS overnight before being treated with DCDT2980S or the control anti-gD-drug conjugate. Each conjugate was added to experimental wells at a final concentration of 50, 16.7, 5.5, 1.8, 0.61, 0.2, 0.067, 0.022, or 0.007 $\mu\text{g}/\text{mL}$. For MMAE, a final concentration of 200, 40, 8, 1.6, 0.32, 0.064, 0.0128, 0.0026, and 0.00051 nmol/L was tested with control wells receiving medium alone. After 72-hour incubation at 37°C , cell viability was measured using the Cell-titer-Glo Luminescent Cell Viability Assay (Promega Corp.). The concentration of DCDT2980S or MMAE resulting in the 50% inhibition of cell viability was calculated from a 4-variable curve analysis and was determined from a minimum of 3 independent biologic replicate experiments.

Xenograft experiments

Xenograft experiments were conducted as previously described (15). Briefly, all animal studies were conducted in compliance with NIH (NIH, Bethesda, MD) guidelines for the care and use of laboratory animals and were approved by the Institutional Animal Care and Use Committee (IACUC) at Genentech, Inc. Cells were inoculated subcutaneously into the flanks of female CB17 ICR severe combined immunodeficient (SCID) mice. When mean tumor size reached desired volume, the mice were divided into groups of 7 to 9 mice with the same mean tumor size and dosed intravenously via the tail vein with ADCs or antibodies. Rituximab was dosed at 30 mg/kg intraperitoneally (i.p.), which is above the maximum efficacious dose. CHOP (single i.v. injection of 30 mg/kg cyclophosphamide, 2.475 mg/kg doxorubicin, 0.375 mg/kg vincristine, and oral dosing of 0.15 mg/kg prednisone once a day for 5 days) was dosed to the maximum tolerated dose defined as the dose, where a 5% weight loss in the animals was observed.

Pharmacokinetic study in SCID mice

The pharmacokinetic study in SCID mice was approved by the IACUC at Genentech, Inc. Female SCID mice received a single intravenous dose of 0.5 or 5 mg/kg DCDT2980S via the tail vein ($n = 20/\text{group}$). Blood samples were collected via retro-orbital bleeds conducted on alternating eyes and the terminal blood sample was collected via cardiac stick from each animal in each dosing group at the following time points: predose; 5 minutes; 1, 6, and 24 hours; and 2, 3, 4, 7, 10, 14, 21, and 28 days postdose, and processed to collect serum. Three blood samples were taken from each mouse and there were 4

mice per time point. Serum concentration-time data were used to estimate relevant pharmacokinetic parameters.

Multiple dose toxicity and toxicokinetics study in cynomolgus monkeys

The toxicity and toxicokinetics study in cynomolgus monkeys was approved by the IACUC and conducted at Covance Laboratories, Inc. (Madison, WI). Animals were dosed intravenously every 3 weeks for a total of 5 doses on study days 1, 22, 43, 64, and 85 with vehicle or DCDT2980S at 1, 3, or 5 mg/kg and were necropsied on day 92 (3 animals/sex/group), day 127 (2 animals/sex/group), or after confirmation of B-cell recovery on day 232 (2 animals/sex/group). Blood was collected prestudy and at selected time points throughout each study for analyses of hematology, serum chemistry, coagulation, toxicokinetics, antitherapeutic antibodies, and measurement of circulating lymphocyte populations by flow cytometry. In addition, ophthalmologic and physical examinations were conducted during the predose phase, and at the end of the first and last dose cycles as applicable. Cardiovascular safety pharmacology endpoints were also evaluated over the course of the study using electrocardiogram external leads. At necropsy, organ weights were measured on select organs and tissues were thoroughly examined by gross and microscopic examination.

Antitumor efficacy study in mice bearing B₂2 and WSU-DLCL2 human non-Hodgkin lymphoma xenografts

The efficacy studies in mice were approved by the IACUC at Genentech, Inc. Female C.B.-17 SCID mice (8–10 week old) were injected with 20 million human non-Hodgkin lymphoma B₂2 or WSU-DLCL2 cells, suspended in 0.2 mL of Hank's balanced salt solution, subcutaneously in the right flank. When tumors reached the desired volume, mice were randomized into 9 groups ($n = 9\text{--}10/\text{per group}$). Mice bearing B₂2 xenografts received a single intravenous dose of vehicle (control group), CNJ1135 (a nonbinding control MC-vc-MMAE conjugate) at 4 mg/kg , MCDT2219A (unconjugated anti-CD22 antibody) at 4 mg/kg , or DCDT2980S (treatment groups) at doses of 0.1, 0.5, 1, 1.5, 2, and 4 mg/kg . Mice bearing WSU-DLCL2 xenografts received a single intravenous dose of vehicle (control group), CNJ1135 (a nonbinding control MC-vc-MMAE conjugate) at 16 mg/kg , MCDT2219A (unconjugated anti-CD22 antibody) at 16 mg/kg , or DCDT2980S (treatment groups) at doses of 1, 2, 4, 8, 12, and 16 mg/kg . Tumors were measured twice each week for the duration of the study using UltraCal-IV calipers and tumor volume was calculated using the following formula: Tumor volume (mm^3) = (length \times width²) \times 0.5. The results were plotted as mean tumor volume \pm SEM of each group over time. Tumor growth inhibition (TGI) as a percentage of vehicle was calculated using the following formula: %TGI = $100 \times [1 - (\text{AUC}_{\text{treatment}}/\text{day} \div \text{AUC}_{\text{vehicle}}/\text{day})]$. Partial response (PR) was defined as a tumor regression of $> 50\%$ but

< 100% of the starting tumor volume, and complete response (CR) was defined as 100% tumor regression (i.e., no measurable tumor) on any day during the study. Time to tumor doubling (TTD) was defined as the time in days for a tumor to double in volume from its initial volume on day 0. Student *t* test was used to evaluate the difference in TTD distributions between groups with a $P \leq 0.05$ to be significant.

Bioanalysis of serum samples from pharmacokinetic and toxicokinetic studies

After administration of DCDT2980S, total antibody (conjugated and unconjugated anti-CD22 antibody) concentrations were analyzed in serum by 2 ELISAs. For serum samples from the pharmacokinetic and toxicokinetic studies in cynomolgus monkeys, microtiter plates were coated with an anti-complementarity determining region antibody against anti-CD22 and incubated overnight, followed by blocking. DCDT2980S standards, controls, and samples were added to the coated plate and incubated for 2 hours to allow for binding. After washing, sheep anti-human IgG conjugated to horseradish peroxidase was added, incubated for 1 hour, and then washed again. 3,3',5,5'-tetramethylbenzidine (TMB) substrate (Kirkegaard and Perry Laboratories, Inc.) was used for detection and absorbance was measured at 450 nm against a reference wavelength of 620 or 630 nm. The minimum quantifiable concentration of the assay was determined to be 80 ng/mL. For serum samples, from the pharmacokinetic study in severe combined immunodeficient mice (SCID) mice, anti-CD22 standards, and samples diluted in sample diluent were incubated for 2 hours with biotinylated sheep anti-human IgG antibody (Genentech, Inc.) and goat anti-human IgG antibody conjugated to horseradish peroxidase in either micronic tubes (National Scientific) or polypropylene round-bottom plates (Corning Costar) to form a bridging complex. Complexed samples were transferred to NeutrAvidin-coated plates (Thermo Fisher Scientific Inc.) and incubated for 1 hour. After washing, the detection step was carried out using TMB substrate (Kirkegaard and Perry Laboratories, Inc.). Absorbance was measured at 450 nm against a reference wavelength of 620 nm. The minimum quantifiable concentration of the assay was determined to be 63 ng/mL.

Pharmacokinetic data analysis

Serum concentration–time profiles were used to estimate the following pharmacokinetic parameters in mouse and monkey, using noncompartmental analysis (WinNonlin, version 5.2.1; Pharsight Corporation): total drug exposure defined as area under the serum concentration–time curve extrapolated to infinity (AUC_{inf}), area under the concentration–time curve from time 0 to TK day 21 (AUC_{0-21}), area under the concentration–time curve from TK day 84 to TK day 105 (AUC_{105}), and observed maximum serum concentration (C_{max}). A naïve pooled approach was used in mouse to provide one estimate for

each dose group, whereas in monkey, each animal was analyzed separately and results for each dose group were summarized as mean \pm SD.

Results

Generation and characterization of DCDT2980S

The antibody anti-CD22 10F4 has been previously identified as an antibody to CD22 that is particularly effective as an ADC compared with other anti-CD22 antibodies when tested in xenograft models (6). The humanized form of 10F4 (MCDT2219A; Hu10F4; ref. 6) was conjugated to MC-vc-PAB-MMAE though the interchain disulfide cysteines (Fig. 1A) as previously described (14). Hydrophobic interaction chromatography (HIC) analysis of DCDT2980S to detect conjugated antibody showed that the average drug to antibody ratio (DAR) for DCDT2980S was 3.6 and consisted of 5% 0-drug, 28% 2-drug, 49% 4-drug, 14% 6-drug, and 3% 8-drug species (Fig. 1B). The antibody MCDT2219A binds cynomolgus monkey and human CD22 but not rat and mouse CD22 (6; Supplementary Fig. S1). The ADC DCDT2980S showed a high binding affinity to human CD22 ($K_d = 1.7 \pm 0.2$ nmol/L) by equilibrium binding similar to that of MCDT2219A. Binding affinity of DCDT2980S was similar between cynomolgus monkey ($K_d = 1.8 \pm 0.1$ nmol/L) and human.

Surface CD22 and sensitivity to MMAE are poor predictors of sensitivity to DCDT2980S *in vitro*

To test the efficacy and reveal parameters that could determine sensitivity to DCDT2980S, we assessed cell viability in a large panel of 35 NHL cell lines (Supplementary Table S1). The degree of sensitivity to DCDT2980S and an isotype control anti-gD-vcMMAE was determined from a dose–response curve of 0–50 μ g/mL and IC_{50} values were calculated (Supplementary Table S1). To ensure that the IC_{50} values calculated were specific to DCDT2980S, we compared IC_{50} values with that of the isotype control anti-gD-vcMMAE. In most of the cell lines that expressed surface target, the IC_{50} of anti-gD-vcMMAE was much greater than the IC_{50} of DCDT2980S; however, 5 cell lines had similar IC_{50} for targeted and control ADC (Supplementary Table S1). These data show that DCDT2980S has very potent and broad activity across a large panel of NHL cell lines. As surface expression levels of CD22 might be an important driver of response to DCDT2980S, we conducted flow cytometry across the panel of NHL cell lines. We then assessed whether there was a correlation with the IC_{50} values obtained with DCDT2980S (Fig. 2A). The overall correlation was low but statistically significant ($R^2 = 0.23$, $P = 0.003$). However, the data suggest that while the higher expressing cell lines (MFI >1,000) predict a sensitive cell line ($IC_{50} < 5$ μ g/mL); cell lines that express lower levels of CD22 are not predictive of response. That is, cell lines with low levels of CD22 could either be quite sensitive to DCDT2980S or comparatively resistant. We also examined how sensitivity of the cell line to MMAE and DCDT2980S correlated (Fig. 2B) and found a moderate

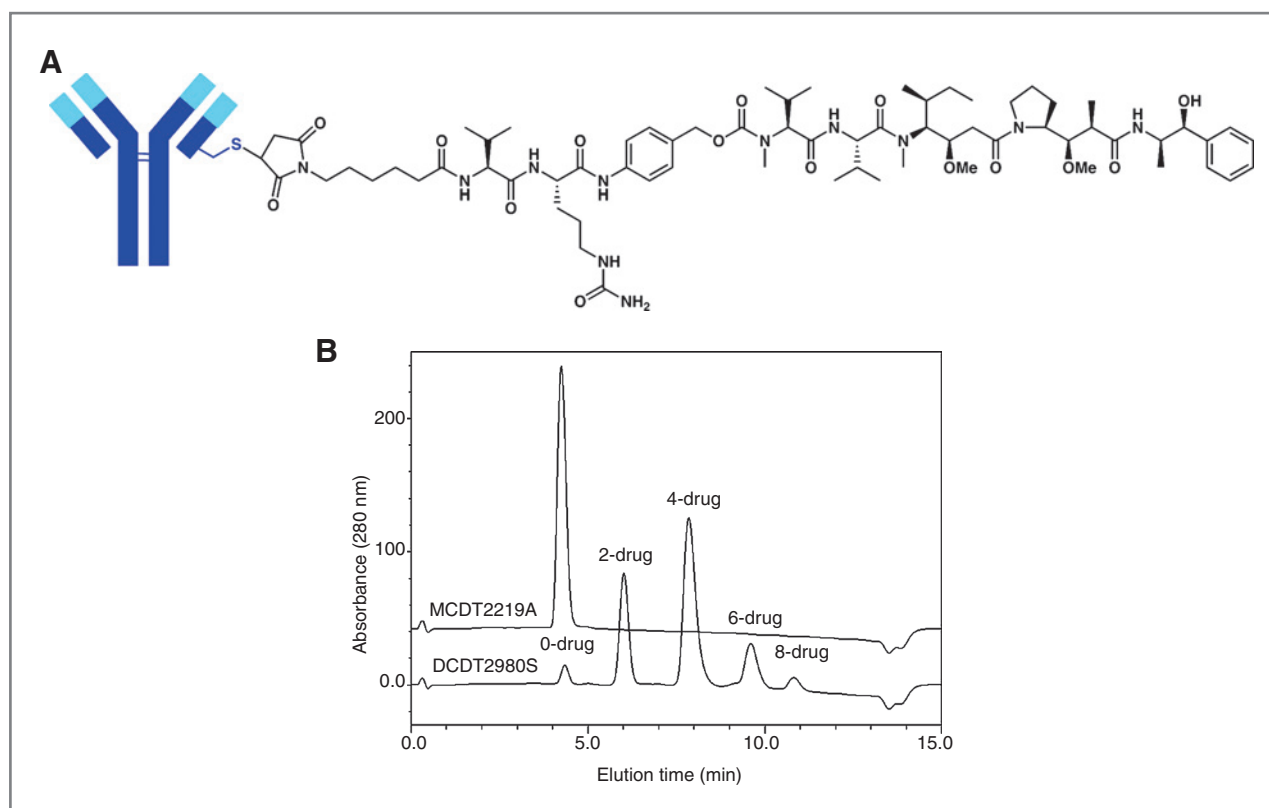


Figure 1. Description of DCDT2980S. A, structure of DCDT2980S. Only one MC-vc-MMAE attached to an interchain disulfide bond linker drug is shown for clarity. B, HIC chromatogram showing the drug distribution of DCDT2980. MCDT2219A, the unconjugated antibody is shown for comparison.

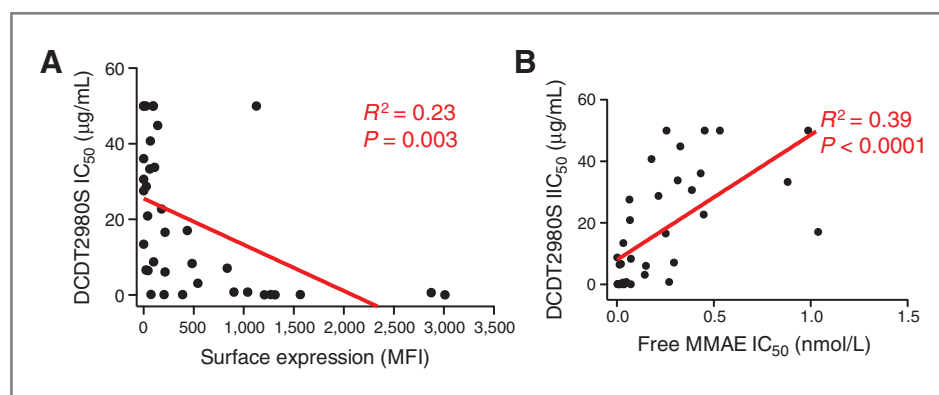
and statistically significant correlation ($R^2 = 0.39$, $P < 0.0001$). These data suggest that sensitivity to the free drug and the amount of surface target effect how a cell line responds to DCDT2980S *in vitro* but neither is a predictor of response.

Efficacy of DCDT2980S in xenograft models of B-cell lymphoma

In addition to testing the activity of DCDT2980S *in vitro*, we tested the activity of DCDT2980S *in vivo* using xenograft tumor models with a wide range of expression of CD22. We evaluated the expression level of CD22 in

several xenograft models and found the expression level of CD22 changed when grown *in vivo* compared with the expression levels when grown in culture (Fig. 3). We selected 2 models for efficacy studies, BJAB for its relatively low expression, (91% of primary tumors have greater surface expression) and WSU-DLCL2 for its relatively high *in vivo* expression of CD22 (8% of primary tumors have greater surface expression) (Fig. 3). *In vitro*, these cell lines are equally sensitive to free drug ($IC_{50} = 0.07$ nmol/L, Fig. 2 and Supplementary Table S1). Mice bearing BJAB tumors (volume range of 160–285 mm³) were given a single dose of vehicle; DCDT2980S at 0.1,

Figure 2. Efficacy of DCDT2980S *in vitro*. *In vitro* cell killing (IC_{50} , μ g/mL) of 35 non-Hodgkin lymphoma cell lines by DCDT2980S as compared with surface expression of CD22 (mean fluorescence intensity, MFI; A) and sensitivity to free MMAE (B).



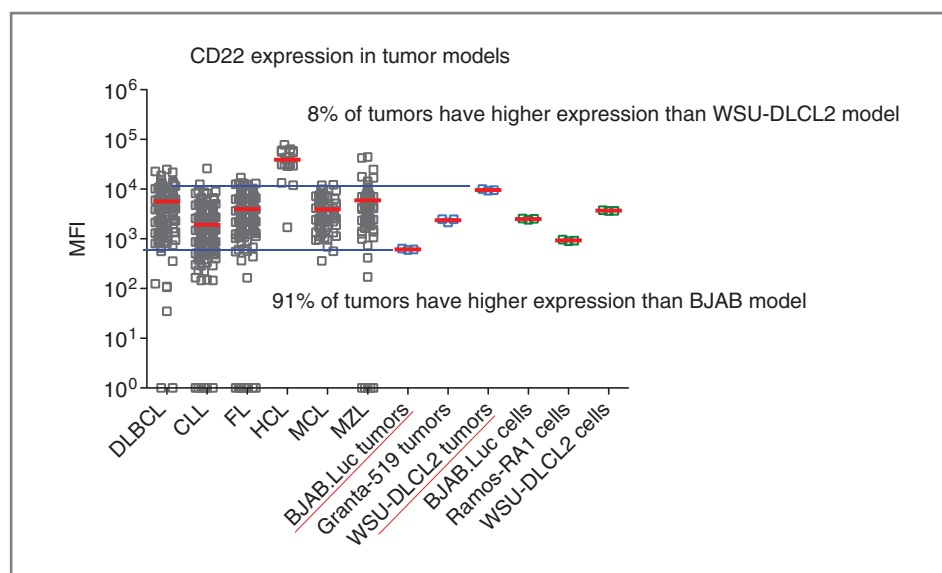


Figure 3. Flow cytometry analysis of CD22 expression on NHL patient samples compared with xenograft tumors and cell lines. Surface expression of CD22 was assessed by FACS (mean fluorescence intensity, MFI) on primary tumor samples from patients with CLL ($n = 349$), DLBCL ($n = 158$), FL ($n = 236$), HCL ($n = 16$), MCL ($n = 66$), and MZL ($n = 78$) as well as on xenograft tumors and cell lines. Red lines show the median of each patient population.

0.5, 1, 1.5, 2, or 4 mg/kg; MCDT2219A (unconjugated DCDT2980S) at 4 mg/kg; or a isotype control (nonbinding) conjugate (CNJ1135) at 4 mg/kg (Fig. 4A). On the basis of the comparisons of tumor growth inhibition (TGI) and time to tumor doubling (TTD), DCDT2980S showed clear dose-dependent inhibitory activity versus the vehicle group at dose levels >0.5 mg/kg ($P < 0.0001$). Of the 10 mice receiving 1.5 mg/kg DCDT2980S, 4 had PRs and 6 had CRs. DCDT2980S at a dose of ≥ 2 mg/kg reached the maximal efficacy, resulting in CRs in all treated mice. The inhibitory effects of a single dose of DCDT2980S were durable, such that 6 of 10 mice receiving 1.5 mg/kg DCDT2980S and all the mice given ≥ 2 mg/kg DCDT2980S maintained CRs until the end of study. MCDT2219A (the unconjugated anti-CD22 antibody) at 4 mg/kg did not have an effect on tumor growth. The nonbinding conjugate CNJ1135 at 4 mg/kg had a minimal effect on tumor growth. Low level of activity of the control conjugate might be due to a low level of CD22-independent delivery of MMAE to tumor cells; however, activity from the group given DCDT2980S at the matching dose level was substantially superior to that from the group given CNJ1135.

Pilot experiments with the tumor xenograft model of human diffuse large B-cell lymphoma WSU-DLCL2 indicated that this model that was more resistant to DCDT2980S; therefore, tumor bearing mice (volume range of 200–325 mm³) were given a single dose of vehicle; DCDT2980S at 1, 2, 4, 8, 12, or 16 mg/kg; MCDT2219A at 16 mg/kg; or a control (nonbinding) conjugate at 16 mg/kg (Fig. 4B). On the basis of comparisons of TGI and TTD, DCDT2980S showed clear dose-dependent inhibitory activity versus the vehicle group at dose levels greater than 2 mg/kg ($P < 0.0001$). Four of 9 mice given 8 mg/kg DCDT2980S and 7 of 9 mice given 12 mg/kg DCDT2980S had PRs. Finally, DCDT2980S at 16 mg/kg exhibited the greatest efficacy, with all treated mice experiencing tumor regression (one PR and 8 CRs).

MCDT2219A (unconjugated DCDT2980S) at 16 mg/kg did not have an effect on tumor growth. The nonbinding conjugate CNJ1135 at 16 mg/kg had a modest effect on tumor growth, possibly due to a low level of CD22-independent delivery of MMAE to tumor cells or non-specific uptake of the ADC, and was not unexpected at this high level. TGI from the group given DCDT2980S at the matching dose level was substantially superior to that from the group given CNJ1135. As in the *in vitro* study, a lower level CD22 of expression did not predict lower activity of DCDT2980S in the *in vivo* study.

Safety profile of DCDT2980S in cynomolgus monkey

Administration of DCDT2980S in mouse xenograft models did not seem to negatively affect the mice since they appeared healthy and gained weight at all dose levels. However, as mice are particularly tolerant of microtubule-inhibiting drugs (16) and DCDT2980S does not bind mouse or rat CD22, rodents are not an appropriate model to test the safety of DCDT2980S. DCDT2980S binds cynomolgus monkey and human CD22 with almost equal affinity (Supplementary Fig. S1) so cynomolgus monkey was chosen as the relevant experimental animal for evaluating the tolerability of DCDT2980S.

Cynomolgus monkeys were intravenously administered DCDT2980S at 1, 3, or 5 mg/kg every 3 weeks for 5 doses. Doses up to 5 mg/kg were well tolerated with no adverse effects on body weight or clinical evidence of toxicity. Notable findings associated with DCDT2980S exposure included reversible bone marrow toxicity and associated hematopoietic changes. Specifically, monkeys were observed with dose-dependent reversible neutropenia (Fig. 5A) and reticulocytopenia (Fig. 5B) at 3 and 5 mg/kg. We also detected minor decreases in erythrocytes, hemoglobin, and hematocrit at 3 and 5 mg/kg, and corresponding bone marrow hypocellularity at all doses

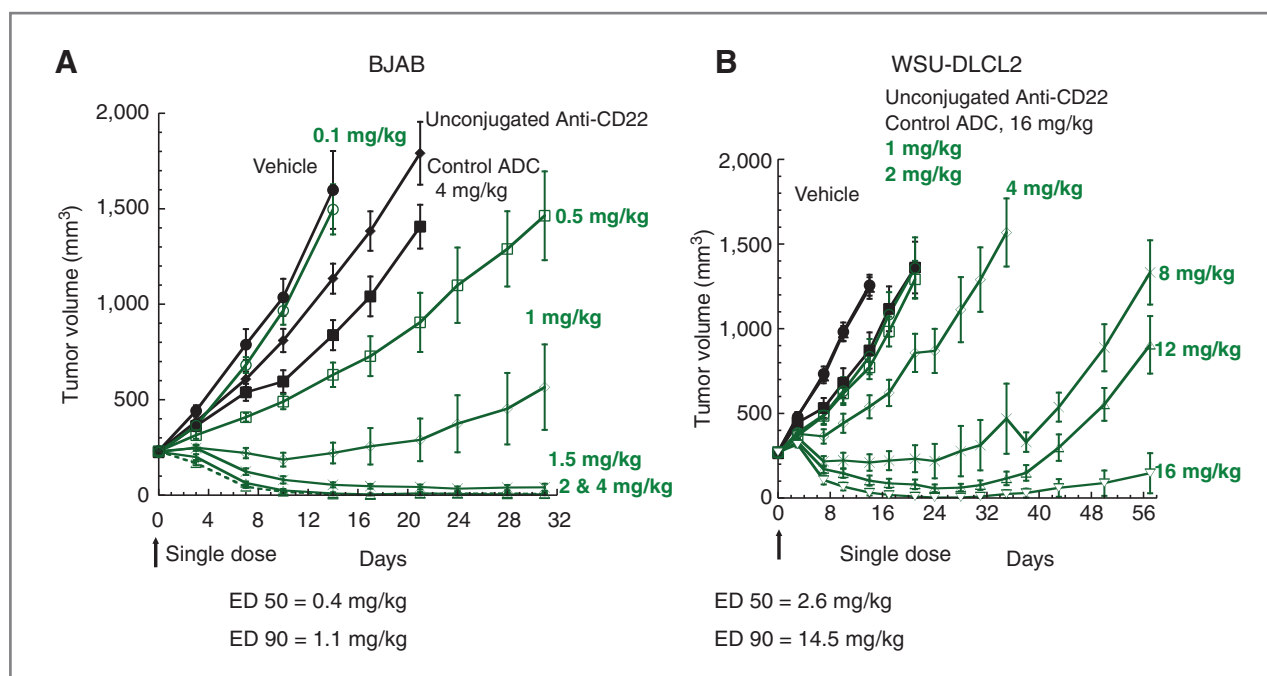


Figure 4. Efficacy of DCDT2980S in tumor xenograft models. Tumor growth was plotted as mean (\pm SEM) tumor volume of each group receiving a single intravenous dose of vehicle, CNJ1135 (nonbinding control conjugate), MCDT2219A (unconjugated anti-CD22), or DCDT2980S over the duration of the study. A, BJAB xenografts ($n = 10$ mice/group) with an average starting tumor volume of 230 mm³ were treated with the doses indicated. B, WSU-DLCL2 xenografts ($n = 9$ mice/group) with an average starting tumor volume of 270 mm³ were treated with the doses indicated.

(data not shown). No cardiovascular, respiratory, renal, gastrointestinal, neurologic, or ophthalmic abnormalities were observed at any dose.

Pharmacokinetics of DCDT2980S in mice and monkeys

In mice, total antibody exposure in the area under concentration–time curve in serum extrapolated to infinity (AUC_{inf}) following single intravenous administration of 0.5 mg/kg and 5 mg/kg of DCDT2980S was 72.1 day \cdot μ g/mL and 821 day \cdot μ g/mL, respectively, suggesting a dose-proportional pharmacokinetic behavior.

In cynomolgus monkeys, exposure of total antibody increased slightly more than dose proportionally from 1 to 3 mg/kg, and dose proportionally from 3 mg/kg to 5 mg/kg. The exposure of last dose interval (AUC_{84-105}) at 3 and 5 mg/kg was higher than that of the first dose interval (AUC_{0-21}), due to depletion of the target B cells up DCDT2980S upon treatment (F.K. Fuh and M. Williams). Thus, concentration- and time-dependent pharmacokinetics of DCDT2980S were observed in cyno, as expected.

To gain a better understanding of the therapeutic potential of DCDT2980S, we used a strategy that assessed the efficacy of DCDT2980S in mouse xenograft models at an exposure (AUC) consistent with the highest non-severely toxic dose (HNSTD) in cynomolgus monkeys. From the HNSTD of 5 mg/kg in the multiple dose cyno toxicity study we calculated an AUC_{84-105} (Table 1), representing the exposure to DCDT2980S after a single

intravenous dose. Using this exposure value and mouse pharmacokinetic data, it was determined that a mouse dose of 4 mg/kg would provide similar DCDT2980S exposure in mice as the dose achieved at the cyno HNSTD (628 ± 71.6 day \cdot μ g/mL). This dose level, 4 mg/kg, has been shown to be efficacious in multiple xenograft models (Figs. 4 and 6) suggesting that efficacious DCDT2980S exposures can be achieved at doses that are well tolerated.

Comparison of the activity of DCDT2980S standard of care *in vivo*

As we had determined doses in mice that resulted in exposures that might be achievable in humans, we invested how the activity of DCDT2980S compared with current standards of care in xenograft models. The current front-line standard of care for most NHLs is a combination of rituximab (anti-CD20 antibody) cyclophosphamide, doxorubicin, vincristine and prednisone (R-CHOP). To compare the activity DCDT2980S to R-CHOP and extend our understanding of the *in vivo* efficacy of DCDT2980S we assessed the activity of DCDT2980S in Ramos-RA1 and Granta-519 lymphoma models. In these studies, we compared the activity of a single dose of DCDT2980S with a single cycle of CHOP, rituximab, or R-CHOP. Rituximab was given above the maximum efficacious dose and CHOP was given close to the maximum tolerated dose for mice (15). As the exposure equivalent of the maximum tolerated dose of DCDT2980S was approximately 4 mg/kg for a single dose exposure, we dosed DCDT2980S once at 5 mg/kg as top end of our exposure

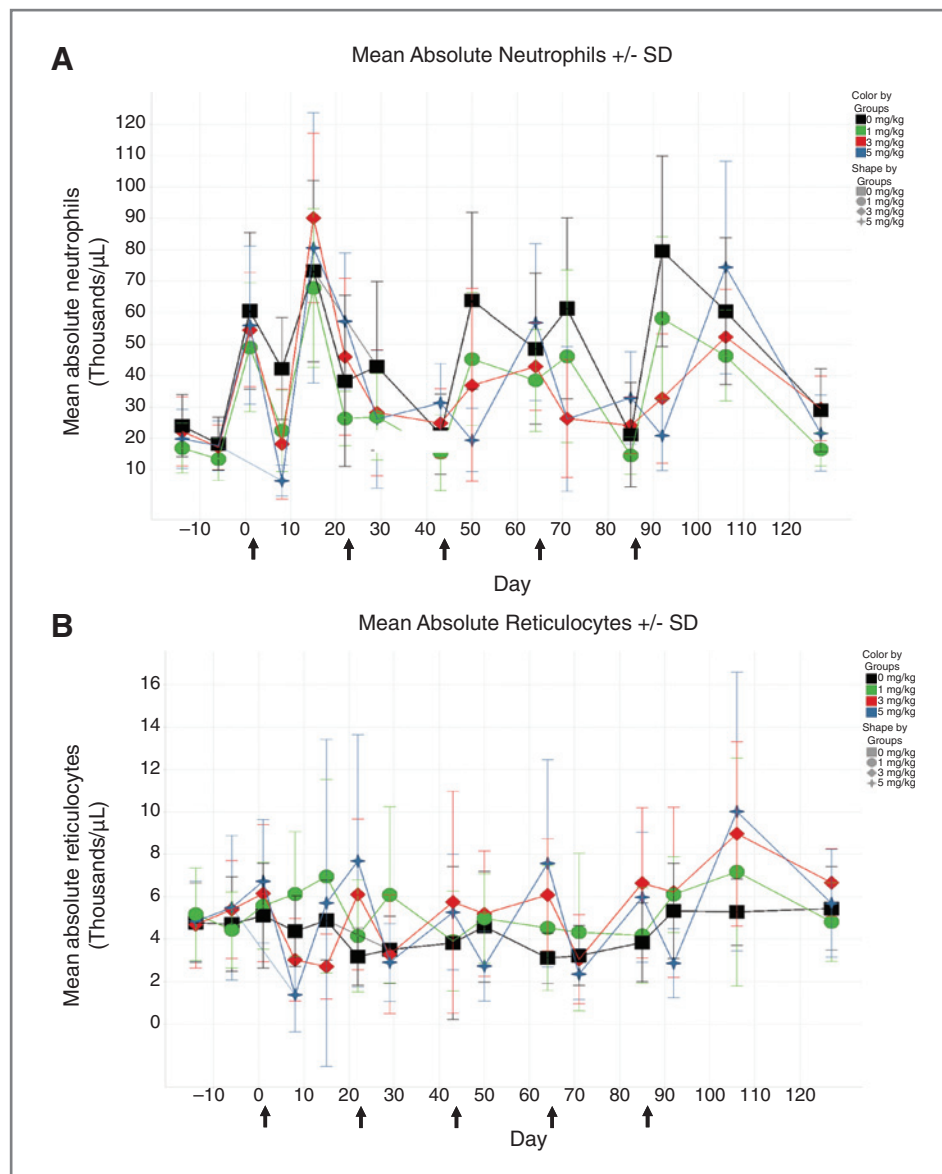


Figure 5. Effect of DCDT2980S on selected hematology in cynomolgus monkeys. The effects of the DCDT2980S dosed every 3 weeks 5 times (arrows) with the indicated amounts on neutrophils (A) and reticulocytes (B). Error bars represent SD.

and 2 mg/kg once to provide a very conservative dose. In the Granta519 model, DCDT2980S was substantially more effective than R-CHOP in inhibiting the tumor growth (Fig. 6A; $P < 0.0001$). On the basis of the comparisons of TGI and TTD, DCDT2980S showed clear inhibitory activity versus the vehicle group for the 2 dose levels tested ($P < 0.0001$). DCDT2980S at 2 and 5 mg/kg produced a TGI of 120% and 126%, and ultimately led to sustained tumor regression in all treated mice. Seven of the 9 mice given 2 mg/kg DCDT2980S and all of the mice given 5 mg/kg DCDT2980S maintained CRs until the end of study, day 28 (see Fig. 6). In contrast, the dose of CHOP or R-CHOP delayed tumor growth and did not achieve any tumor regression, with a TGI of 79% and 90%, respectively, and a TTD of 12 and 13.5 days. Rituximab alone at 30 mg/kg had a modest effect on delaying tumor growth. The nonbinding conjugate CNJ1135, given at 5 mg/kg, had a noticeable

effect on tumor growth, yielding a TGI of 68% and a TTD of 10 days. Activity due to a low level of CD22-independent delivery of MMAE to tumor cells is not unexpected at this dose level. Even so, the TGI from the group given DCDT2980S at the matching dose level was still superior to that from the group given CNJ1135.

In the Ramos RA1 model, a single dose of DCDT2980S resulted in dose-dependent inhibition of tumor growth (Fig. 6). On the basis of the comparisons of TGI and TTD, DCDT2980S showed clear inhibitory activity versus the vehicle group for the 2 dose levels tested ($P \leq 0.0005$). DCDT2980S at 2 mg/kg and R-CHOP had comparable activity, with a TGI of 76% and 73%, respectively, and a TTD of 7 and 6.5 days, compared with a TTD of 2.5 days in the vehicle group. The effects of 5 mg/kg DCDT2980S were more pronounced, with a TGI of 112%, and ultimately led to sustained tumor regression in all treated

Table 1. Group mean (\pm SD) pharmacokinetic parameters of total antibody after a single intravenous administration of DCDT2980S to SCID mice and multiple (q3w x 5) intravenous administrations of DCDT2980S to cynomolgus monkeys

Dose (mg/kg)	Mouse (single dose)		Cynomolgus monkey (q3w x 5)			
	C_{max} (μ g/mL)	AUC_{inf} (μ g \cdot day/mL)	First dose		Last dose	
			C_{max} (μ g/mL)	AUC_{0-21} (μ g \cdot day/mL)	C_{max} (μ g/mL)	AUC_{84-105} (μ g \cdot day/mL)
1	NA	NA	24.9 \pm 2.97	62.9 \pm 6.06	26.9 \pm 1.13	76.8 \pm 7.52
3	NA	NA	87.8 \pm 11.0	259 \pm 24.1	108 \pm 13.4	400 \pm 51.8
5	134	821	134 \pm 18.1	388 \pm 39.6	159 \pm 13.2	628 \pm 71.6
0.5	11.1	72.1			NA	
4 (estimated)	NA	628 \pm 71.6			NA	

Abbreviations: q3w x 5, every 3 weeks for 5 doses; NA, not available.

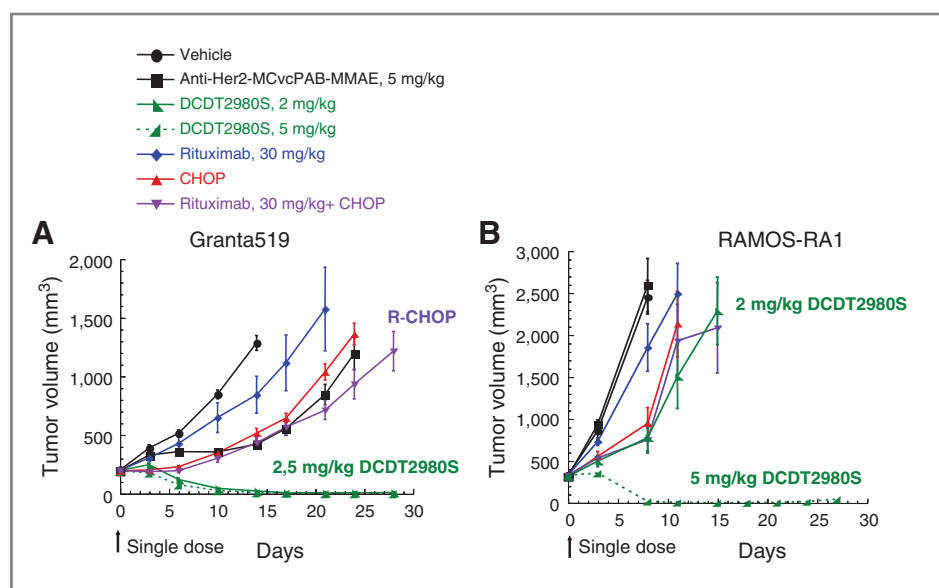
mice. Of the 7 mice given 5 mg/kg DCDT2980S, 5 maintained CRs until the end of the study. As expected, the nonbinding conjugate CNJ1135, given at 5 mg/kg, did not have an effect on tumor growth. These data suggest that DCDT2980S could be very effective compared with standard of care. At a minimum, they suggest that the excellent tumor responses we observe are not due to an extreme sensitivity of the models to antibody therapy or chemotherapy.

Discussion

Here, we describe DCDT2980S, an anti-CD22-MC-vc-PAB-MMAE ADC, and its preclinical safety and efficacy. We found that DCDT2980S was broadly active *in vitro* and that comparatively low amounts of target were not a barrier to efficacy. Furthermore, the *in vitro* activity translated to activity of DCDT2980S in *in vivo* models of NHL. As the antibody is not cross-reactive to rodents and mice

are uniquely insensitive to auristatin-type drugs (16), cynomolgus monkeys were used to assess the DCDT2980S safety profile. DCDT2980S was well tolerated in cynomolgus monkeys with neutropenia as a predominant safety finding. The pharmacokinetics of DCDT2980S in SCID mice where efficacy studies were conducted seemed to be dose proportional. In cynomolgus monkeys, the pharmacokinetics of DCDT2980S seemed to be slightly nonlinear in the dose range of 1 to 3 mg/kg and became dose proportional in the dose range of 3 to 5 mg/kg of DCDT2980S. Thus, the contribution of B-cell (CD22)-mediated clearance to total clearance at the dose range of 1 to 3 mg/kg seemed to be moderate. In mouse and cynomolgus monkey pharmacokinetic studies, the concentrations of the conjugate (DCDT2980S) were also measured (data not shown). Comparison of the total antibody and DCDT2980S concentrations over time assessed the *in vivo* stability of the conjugate. The DCDT2980S serum

Figure 6. *In vivo* efficacy of DCDT2980S compared with standard of care. Mouse xenograft models of NHL with an average starting tumor volume of 200–300 mm³ treated with a single dose of 2 or 5 mg/kg DCDT2980S compared with a single treatment of rituximab, CHOP, Rituximab plus CHOP. Tumor growth was plotted as mean (\pm SEM) tumor volume of each group. A, Granta-519 xenografts with 9 mice treated as indicated. B, Ramos-RA1 xenografts with 7 mice per group were treated as indicated.



concentration decreased biexponentially, in a manner similar to total antibody, suggesting that MMAE is not rapidly released from DCDT2980S.

To understand the potential efficacy of DCDT2980S at drug exposures that were tolerated in cynomolgus monkeys, we translated a single dose exposure found to be safe in a 5 dose cynomolgus monkey study to our mouse models and found that an exposure of a single dose would be equivalent to approximately 4 mg/kg in mice. This would be an efficacious dose in all 4 of the xenograft models we tested. Again, levels of surface CD22 that were low compared with the levels of CD22 expression found in primary NHL tumors were not a barrier to efficacy. The BJAB and WSU-DLCL2 models had very different sensitivities to the DCDT2980S, ED₉₀ of 1.1 versus 14.5 mg/kg respectively; however, the BJAB model had lower surface expression of CD22 and the cell lines had equal sensitivity to MMAE *in vitro*. The drivers of *in vivo* sensitivity to DCDT2980S are unclear at this point; however, our data suggest that DCDT2980S could be broadly active and not limited to patients with high CD22 expression. The observation that R-CHOP combination therapy dosed at near the maximum tolerated dose is not as efficacious as relevant doses of the ADC suggest that the excellent *in vivo* activity we observed is not due to a general sensitivity to chemotherapy in our xenograft models. Assuming that the cynomolgus monkey is a reasonable model for human pharmacokinetic properties and tolerability of DCDT2980S, DCDT2980S could be of therapeutic use in the majority of patients with NHL. This conclusion is also supported by our current clinical understanding of the target and linker-drug. CD22 is a clinically validated target for both monoclonal antibody therapy and ADC therapy (17, 18) and MC-vc-MMAE is the linker drug used in the anti-CD30 ADC brentuximab vedotin, which is approved for the treatment of patients with Hodgkin lymphoma after failure of autologous stem cell transplant (ASCT) or after failure of at least 2 prior multiagent chemotherapy regimens. The objective response rate in the brentuximab vedotin in patients with Hodgkin lymphoma was 75% suggesting that the linker-drug technology used in DCDT2980S has the potential to be broadly effective in the treatment of NHL at tolerated dose (19). On the basis of the work and rationale described here, DCDT2980S is being tested in phase I trials for the treatment of NHL and CLL.

phoma was 75% suggesting that the linker-drug technology used in DCDT2980S has the potential to be broadly effective in the treatment of NHL at tolerated dose (19). On the basis of the work and rationale described here, DCDT2980S is being tested in phase I trials for the treatment of NHL and CLL.

Disclosure of Potential Conflicts of Interest

F. Fuh is employed (other than primary affiliation; e.g., consulting) as a senior research associate in Genentech/Roche. R. de Tute has commercial research support from Genentech. A. Rawstron has a commercial research grant from Genentech. A.S. Jack has commercial research support from Genentech. S. Prabhu is employed (other than primary affiliation; e.g., consulting) as a senior scientist in Genentech Inc.

Authors' Contributions

Concept and design: D. Li, S.-F. Yu, R. Deng, A. Ebens, S. Prabhu, A.G. Polson

Development of methodology: D. Li, B. Zheng, K.R. Kozak, P. Chan, J. McBride, A. Ebens, S. Prabhu

Acquisition of data (provided animals, acquired and managed patients, provided facilities, etc.): D. Li, R. Dere, M. Go, J. Lau, B. Zheng, K. Elkins, D. Danilenko, P. Chan, J. Chuh, X. Shi, F. Fuh, R. de Tute, A. Rawstron, A.S. Jack, D. Dornan, W. Ho, S. Prabhu

Analysis and interpretation of data (e.g., statistical analysis, biostatistics, computational analysis): D. Li, K. Achilles-Poon, S.-F. Yu, R. Dere, J. Lau, B. Zheng, K. Elkins, K.R. Kozak, P. Chan, X. Shi, J. McBride, V. Ramakrishnan, R. de Tute, A. Rawstron, R. Deng, D. Dornan, S. Prabhu

Writing, review, and/or revision of the manuscript: D. Li, K. Achilles-Poon, S.-F. Yu, R. Dere, K. Elkins, D. Danilenko, K.R. Kozak, D. Nazzari, F. Fuh, J. McBride, V. Ramakrishnan, A. Rawstron, Y.-W. Chu, M. Williams, S. Prabhu, A.G. Polson

Administrative, technical, or material support (i.e., reporting or organizing data, constructing databases): D. Li, M. Go, K. Elkins, S. Prabhu

Study supervision: D. Li, K. Achilles-Poon, V. Ramakrishnan, S. Prabhu

Acknowledgments

The authors thank Kristopher Moore, Covance Laboratories for assistance with our safety studies, the Genentech *in vivo* cell culture group, Josefa Chuh for ELISA and pharmacokinetic assay assistance, and Jeffery Gorrell for drug production.

The costs of publication of this article were defrayed in part by the payment of page charges. This article must therefore be hereby marked *advertisement* in accordance with 18 U.S.C. Section 1734 solely to indicate this fact.

Received December 4, 2012; revised March 18, 2013; accepted March 19, 2013; published OnlineFirst April 18, 2013.

References

1. Bagg A. B cells behaving badly: a better basis to behold belligerence in B-cell lymphomas. *Hematology* 2011;2011:330-5.
2. Salles GA. Clinical features, prognosis and treatment of follicular lymphoma. *Hematology* 2007;216-25.
3. Coiffier B, Thieblemont C, Van Den Neste E, Lepage G, Plantier I, Castaigne S, et al. Long-term outcome of patients in the LNH-98.5 trial, the first randomized study comparing rituximab-CHOP to standard CHOP chemotherapy in DLBCL patients: a study by the Groupe d'Etudes des Lymphomes de l'Adulte. *Blood* 2010;116:2040-5.
4. Jemal A, Siegel R, Ward E, Hao Y, Xu J, Thun M. Cancer statistics, 2009. *CA: Cancer J Clin* 2009;59:225-49.
5. Polson AG, Calemine-Fenaux J, Chan P, Chang W, Christensen E, Clark S, et al. Antibody-drug conjugates for the treatment of non-hodgkin's lymphoma: target and linker-drug selection. *Cancer Res* 2009;69:2358-64.
6. Polson AG, Williams M, Gray AM, Fuji RN, Poon KA, McBride J, et al. Anti-CD22-MCC-DM1: an antibody-drug conjugate with a stable linker for the treatment of non-Hodgkin's lymphoma. *Leukemia* 2010;24:1566-73.
7. Polson AG, Yu SF, Elkins K, Zheng B, Clark S, Ingle GS, et al. Antibody-drug conjugates targeted to CD79 for the treatment of non-Hodgkin's lymphoma. *Blood* 2007;110:616-23.
8. Tedder TF, Tuscano J, Sato S, Kehrl JH. CD22, a B lymphocyte-specific adhesion molecule that regulates antigen receptor signaling. *Ann Rev Immunol* 1997;15:481-504.
9. Barclay AN, Brown M, Law SKA, McKinght AJ, Tomlinson MG, Anton van der Merwe P. The leucocyte antigen facts book. San Diego, CA: Academic Press; 1997.
10. Leonard JP, Goldenberg DM. Preclinical and clinical evaluation of epratuzumab (anti-CD22 IgG) in B-cell malignancies. *Oncogene* 2007;26:3704-13.
11. Traczewski P, Rudnicka L. Treatment of systemic lupus erythematosus with epratuzumab. *Br J Clin Pharmacol* 2011;71:175-82.

12. DiJoseph JF, Armellino DC, Boghaert ER, Khandke K, Dougher MM, Sridharan L, et al. Antibody-targeted chemotherapy with CMC-544: a CD22-targeted immunoconjugate of calicheamicin for the treatment of B-lymphoid malignancies. *Blood* 2004;103:1807–14.
13. Zein N, Poncin M, Nilakantan R, Ellestad GA. Calicheamicin gamma 11 and DNA: molecular recognition process responsible for site-specificity. *Science* 1989;244:697–9.
14. Doronina SO, Toki BE, Torgov MY, Mendelsohn BA, Cerveny CG, Chace DF, et al. Development of potent monoclonal antibody auristatin conjugates for cancer therapy. *Nat Biotechnol* 2003;21:778–84.
15. Dornan D, Bennett F, Chen Y, Dennis M, Eaton D, Elkins K, et al. Therapeutic potential of an anti-CD79b antibody-drug conjugate, anti-CD79b-vc-MMAE, for the treatment of non-Hodgkin lymphoma. *Blood* 2009;114:2721–9.
16. Mirsalis JC, Schindler-Horvat J, Hill JR, Tomaszewski JE, Donohue SJ, Tyson CA. Toxicity of dolastatin 10 in mice, rats and dogs and its clinical relevance. *Cancer Chemother Pharmacol* 1999;44:395–402.
17. Leonard JP, Coleman M, Ketas JC, Chadburn A, Furman R, Schuster MW, et al. Epratuzumab, a humanized anti-CD22 antibody, in aggressive non-Hodgkin's lymphoma: phase I/II clinical trial results. *Clin Cancer Res* 2004;10:5327–34.
18. Ogura M, Uchida T, MacDonald DA, Hatake K, Davies A, Sangha R, et al. An open-label, phase I study of R-CVP in combination with inotuzumab ozogamicin in patients with relapsed/refractory CD22-positive B-cell non-hodgkin lymphoma. *Blood (ASH Annual Meeting Abstracts)* 2011;118:3715.
19. Gopal AK, Ramchandren R, O'Connor OA, Beryman RB, Advani RH, Chen R, et al. Safety and efficacy of brentuximab vedotin for Hodgkin lymphoma recurring after allogeneic stem cell transplantation. *Blood* 2012;120:560–8.

Molecular Cancer Therapeutics

DCDT2980S, an Anti-CD22-Monomethyl Auristatin E Antibody–Drug Conjugate, Is a Potential Treatment for Non-Hodgkin Lymphoma

Dongwei Li, Kirsten Achilles Poon, Shang-Fan Yu, et al.

Mol Cancer Ther 2013;12:1255-1265. Published OnlineFirst April 18, 2013.

Updated version Access the most recent version of this article at:
doi:[10.1158/1535-7163.MCT-12-1173](https://doi.org/10.1158/1535-7163.MCT-12-1173)

Supplementary Material Access the most recent supplemental material at:
<http://mct.aacrjournals.org/content/suppl/2013/04/19/1535-7163.MCT-12-1173.DC1>

Cited articles This article cites 17 articles, 9 of which you can access for free at:
<http://mct.aacrjournals.org/content/12/7/1255.full#ref-list-1>

Citing articles This article has been cited by 13 HighWire-hosted articles. Access the articles at:
<http://mct.aacrjournals.org/content/12/7/1255.full#related-urls>

E-mail alerts [Sign up to receive free email-alerts](#) related to this article or journal.

Reprints and Subscriptions To order reprints of this article or to subscribe to the journal, contact the AACR Publications Department at pubs@aacr.org.

Permissions To request permission to re-use all or part of this article, use this link
<http://mct.aacrjournals.org/content/12/7/1255>.
Click on "Request Permissions" which will take you to the Copyright Clearance Center's (CCC) Rightslink site.